Narrow-Line Waveguide Terahertz Time-Domain Spectroscopy of Aspirin and Aspirin Precursors

N. LAMAN, S. SREE HARSHA, and D. GRISCHKOWSKY*

School of Electrical and Computer Engineering, Oklahoma State University, Stillwater, Oklahoma 74078

Low frequency vibrational modes of pharmaceutical molecules are dependent on the molecule as a whole and can be used for identification purposes. However, conventional Fourier transform far-infrared spectroscopy (FT-IR) and terahertz time-domain spectroscopy (THz-TDS) often result in broad, overlapping features that are difficult to distinguish. The technique of waveguide THz-TDS has been recently developed, resulting in sharper spectral features. Waveguide THz-TDS consists of forming an ordered polycrystalline film on a metal plate and incorporating that plate in a parallel-plate waveguide, where the film is probed by THz radiation. The planar order of the film on the metal surface strongly reduces the inhomogeneous broadening, while cooling the waveguide to 77 K reduces the homogeneous broadening. This combination results in sharper absorption lines associated with the vibrational modes of the molecule. Here, this technique has been demonstrated with aspirin and its precursors, benzoic acid and salicylic acid, as well as the salicylic acid isomers 3- and 4-hydroxybenzoic acid. Linewidths as narrow as 20 GHz have been observed, rivaling single crystal measurements.

Index Headings: **THz spectroscopy; Terahertz Time-domain spectroscopy; Far infrared; Waveguide; Aspirin; Benzoic acid.**

INTRODUCTION

The low frequency vibrational modes of a number of pharmaceutical molecules often appear at THz frequencies. These modes are generally not associated with motion of a localized bond, but rather with motion of the molecule as a whole. In addition to internal (intramolecular) modes, many of these molecules exhibit external (intermolecular) modes related to the molecule's motion within a crystalline lattice. Indeed, the crystallinity of a number of pharmaceutical molecules has been measured by observing external vibrational modes.[1–5]

The delocalized nature of the vibrational modes makes the absorption spectrum of a particular molecule unique in principle. However, in practice, both homogeneous and inhomogeneous broadening can obscure spectral lines, causing absorption spectra from different molecules to look similar. There has been some success in the detection and identification of different pharmaceutical molecules,[6] primarily in the area of illicit drugs.[7–9] However, the ability to distinguish among these molecules could be greatly improved by reducing both the homogeneous and inhomogeneous broadening.

Here, we report the reduction of homogeneous and inhomogeneous broadening in the terahertz (THz) absorption spectra of the pharmaceutical compounds of aspirin and its precursors. This reduction in broadening was accomplished by the new technique of waveguide THz time-domain spectroscopy (THz-TDS),[10,11] where an ordered polycrystalline film is formed on a metal plate, which is then incorporated into a parallel-plate waveguide.[11]

Received 11 October 2007; accepted 21 December 2007.

* Author to whom correspondence should be sent. E-mail: daniel.grischkowsky@okstate.edu.

EXPERIMENTAL

Terahertz time-domain spectroscopy is the study of material properties using time-resolved sub-picosecond THz pulses with frequency content between 0.1 and 5 THz.[12] Typically, as shown in Fig. 1, one excites a biased photoconductive semiconductor antenna with an ultrafast laser pulse, resulting in a broadband THz pulse. This THz pulse is collimated by a high-resistivity Si lens and a parabolic mirror, then transmitted through the sample under investigation, and finally refocused onto a gated semiconductor photoconductive antenna, which acts as a detector. Measurement with a frequency resolution of 1 GHz and signal-to-noise (S/N) ratio of 10 000 can be achieved.[13] The entire system is located in an airtight enclosure to mitigate the effects of water vapor on the THz beams.

A high-performance optoelectronic source chip, used to generate pulses of freely propagating THz electromagnetic radiation, is shown in Fig. 1b. The simple coplanar transmission line structure of the chip consists of two 10-μm-wide metal lines separated by 80 μm, fabricated on high-resistivity GaAs. Irradiating the metal-semiconductor interface (edge) of the positively biased line with focused ultrafast laser pulses produces synchronous bursts of THz radiation. This occurs because each laser pulse creates a spot of photocarriers in a region of extremely high electric field. The consequent acceleration of the carriers generates the burst of radiation. A titanium sapphire laser provides the 850 nm, 80 fs excitation pulses at a 100 Mhz repetition rate in a beam with an attenuated average power of 10 mW at the 5 μm diameter excitation spot. The major fraction of the laser-generated burst of THz radiation is emitted into the GaAs substrate in a cone normal to the interface and is then collected and collimated by a crystalline high-resistivity silicon lens attached to the back side of the chip.

The THz radiation detector is an ion-implanted SOS detection chip with the antenna geometry shown in Fig. 1c. The 4 μm wide antenna structure is embedded in a coplanar transmission line consisting of two parallel 2 μm wide aluminum lines separated from each other by 6 μm. The electric field of the focused incoming THz radiation induces a transient bias voltage across the 2 μm gap between the two arms of this receiving antenna, directly connected to a low-noise current amplifier. The amplitude and time dependence of this transient voltage is obtained by measuring the collected charge (average current) versus the time delay between the THz pulses and the Ti:sapphire detection pulses. These pulses in the 10 mW laser detection beam synchronously gate the receiver by driving (closing) the photoconductive switch defined by the 2 μm antenna gap. Simply speaking, the switch is closed by the photocarriers created by the 80 fs laser pulse; the switch then reopens in approximately 600 fs due to the short carrier lifetime in ion-implanted SOS.

The generated THz pulse is shown by the single-scan

0003-7028/08/6203-0319$2.00/0

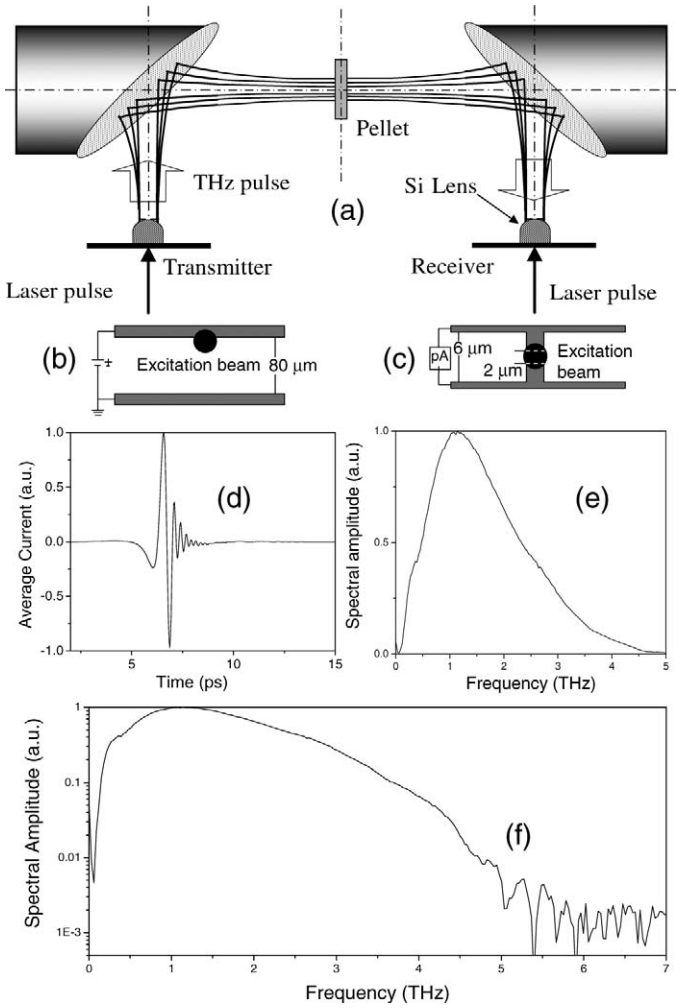

FIG. 1. (**a**) Conventional THz-TDS apparatus. (**b**) THz emitter and (**c**) receiver. (**d**) Normalized typical free-space THz pulse and corresponding amplitude spectrum with both (**e**) linear and (**f**) logarithmic vertical scales.

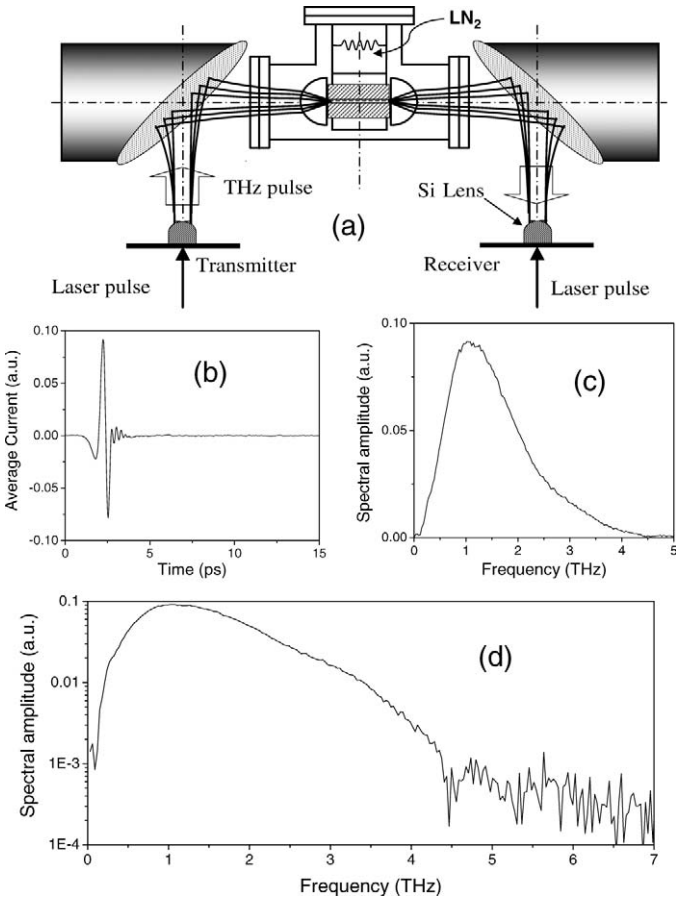

FIG. 2. (**a**) Waveguide THz-TDS apparatus. THz pulse transmitted through 30 mm long Cu waveguide with 50 μm gap normalized to free-space signal in Fig. 1d (**b**) and corresponding amplitude spectrum normalized to free-space spectrum with both (**c**) linear and (**d**) logarithmic vertical scales.

measurement in Fig. 1d with a max to min 300 fs time separation. The max to min normalized amplitude difference of 2.0 is to be compared with the root mean square (rms) amplitude noise of 0.0004, giving an amplitude S/N ratio of 5000. The corresponding amplitude spectrum of this pulse is shown in Fig. 1e. The S/N ratio of the amplitude spectrum is shown in the logarithmic plot of Fig. 1f. Here, the dynamic range or S/N is displayed as 700:1.

The conventional sample preparation technique for both Fourier transform infrared (FT-IR) spectroscopy and THz-TDS is to mix the molecular powder under study with a transparent powder such as polyethylene and press the resulting mixture into a pellet. The pellet comprises crystals with random sizes and orientations embedded in the polyethylene matrix. The transmission spectrum of the pellet is then measured with a conventional THz-TDS apparatus,[12,13] as shown in Fig. 1. Frequently, the pellet is cooled to cryogenic temperatures in order to minimize homogenous broadening. Inhomogeneous broadening is strongly related to the degree of disorder in the sample. Random polycrystalline samples such as pellets have a great deal of disorder, resulting in substantial inhomogeneous broadening. In principle, the least amount of inhomogeneous broadening would result from a sample comprising a single crystal, but this is often inconvenient.

The efficient coupling together with the single TEM-mode high performance of the parallel plate waveguide (PPWG) is a key breakthrough for characterizing sub-wavelength thick sample layers in the THz spectral region.[14,15] Waveguide THz-TDS utilizes THz spatial confinement to sub-wavelength dimensions together with long propagation lengths to dramatically improve the sample filling factor and consequently the sensitivity. For the TEM-mode of parallel plate metal waveguides, the spatial confinement, determined by the separation b between the plates, can be easily $b = \lambda/10$. By comparing the signal from the empty waveguide with that from the waveguide containing the sample layer, one can extract the changes in both amplitude and phase caused by the addition of the layer. Knowing the layer thickness, one can then obtain the absorption and the index of refraction of the layer material. The high sensitivity of this measurement technique is proportional to the ratio between the length and the plate separation of the waveguide.

The quasi-optical coupling of a freely propagating THz beam into the PPWG located at the beam waist of the THz-TDS system (shown in Fig. 2) is surprisingly efficient over the entire bandwidth.[14,15] Compared to the free-space system, the insertion of only the two required cylindrical lenses separated by their focal lengths reduces the amplitude of the transmitted

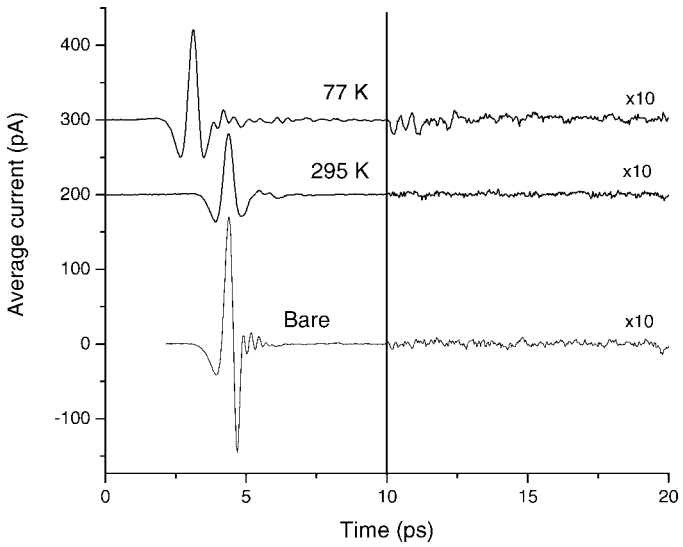

FIG. 3. THz pulses transmitted through bare Cu waveguide and the same waveguide with aspirin film at both 295 K and 77 K. Traces are multiplied by a factor of 10 after 10 ps.

THz pulse by the multiplicative factor $0.4 = 0.8 \times 0.5$, where 0.5 is the Fresnel transmission through the uncoated high-resistivity Si lenses (due to the reflective losses of four surfaces). The factor 0.8 is the quasi-optical amplitude coupling (transmission) through the two confocal lenses. In Fig. 2, the foci of the two lenses were separated by the 30 mm long, 50 μm air-spaced Cu parallel-plate waveguide, for which the amplitude transmission was reduced to $0.18 = 0.45 \times 0.8 \times 0.5$, similar to the situation for the experiments to be described later. The additional factor of 0.45 is mainly due to the waveguide coupling loss with a smaller loss due to waveguide absorption. The input Si lens focuses the incoming THz pulse to an elliptical spot with the minor axis of 150 μm, perpendicular to the waveguide plates, and the linearly wavelength dependent major axis of 9 mm at 1 THz, parallel to the waveguide plates.

The single-scan measured THz pulse transmitted through an empty waveguide is shown in Fig. 2b, for the setup shown in Fig. 2a. Here the pulse amplitude is normalized to the free-space THz pulse of Fig. 1d and shows a reduced amplitude transmission of 0.09, which includes the additional factor of 0.5 due to the strong reflections from the Si windows on the vacuum chamber. The corresponding amplitude spectrum shown in Fig. 2c has been normalized to the free space spectrum of Fig. 1e. The waveguide-transmitted spectrum is shown logarithmically in Fig. 2d. For our experiments, we typically averaged six measurement scans for the pellet measurements and eight scans for the waveguide measurements. The temporal scan length for most of the low-temperature pellet and waveguide measurements was 33 ps, resulting in a frequency resolution of 0.03 THz (1 cm^{-1}). The exception is the measurement of the benzoic acid waveguide, which has a temporal scan length of 66 ps, corresponding to a frequency resolution of 0.015 THz (0.5 cm^{-1}). All of the temporal traces were zero-padded by a factor of 2 before the Fourier transform was performed. However, this acts as an interpolation in frequency and does not increase the frequency resolution.

A characteristic set of THz pulses corresponding to our aspirin measurements are shown in Fig. 3. These are individual scans, showing the quality of the data and the high S/N ratio. The THz pulses at both 295 K and 77 K show ringing corresponding to spectral features, with the longer ringing at 77 K corresponding to sharper spectral features. The temporal shift upon cooling is due to the change of the refractive index of the Si lenses. After this set of experiments, the waveguide was rinsed with methanol without removing the Si lenses, allowing for the measurement of the corresponding bare waveguide.

In our initial demonstration of waveguide THz-TDS,[10] we measured the THz index of refraction and absorption of extremely thin 20 nm water layers on the waveguide plates. More recently, together with Joseph S. Melinger, we have extended the waveguide THz-TDS technique to thin microcrystalline films,[11] for which the inhomogeneous broadening can be minimized. Here the investigated molecule is first deposited on a metal waveguide plate in a manner such that the resulting polycrystalline thin film is ordered relative to the metal surface. The coated plate is then incorporated as one of the plates of the parallel plate waveguide.[11,16,17]

The planar order in this polycrystalline film relative to the metal plate (and hence relative to the THz polarization) can reduce the inhomogeneous broadening significantly compared to the random crystals in the corresponding pellet. In essence, this technique allows one to have order approaching a single crystal sample, but with a much easier to produce polycrystalline film (although not as easy to produce as a pellet). Furthermore, the waveguide can be cooled down to 77 K in order to reduce homogeneous broadening. The reduction of both homogeneous and inhomogeneous broadening can result in considerably narrower absorption lines compared to conventional THz-TDS. This line-narrowing effect has been observed in 1,2- and 1,3-Dicyanobenzene[11,16] and TCNQ,[16] as well as a number of small biological molecules.[17] Not only is the parallel plate waveguide geometry a high-resolution and convenient method to study the ordered polycrystalline film, but it also enhances the amplitude absorbance of the film by approximately a factor of 100,[14] compared to the traditional single transverse pass through the same film thickness.

In addition to the absorption lines sharpening, the overall transmitted spectrum generally increases at 77 K compared with 295 K for both pellets and waveguides, indicating that the broadband background absorption has decreased. For the pellets and films examined here, the transmitted spectra increase by approximately 15 and 30%, respectively. The transmission of a bare waveguide does not increase with reduced temperature.[18]

Aspirin (acetylsalicylic acid) is a very popular and well-studied drug, used primarily as an analgesic, antipyretic, and also for blood thinning (antiplatelet). The purpose of this paper is to demonstrate line-narrowing with waveguide THz-TDS for aspirin and its precursors, benzoic acid and salicylic acid (2-hydroxybenzoic acid). In addition, we have used waveguide THz-TDS to measure 3- and 4-hydroxybenzoic acid, demonstrating clear distinction between the isomers.

All five materials were purchased from Sigma-Aldrich and used without further purification. The pellets were formed by mixing the analyte with a polyethylene powder and compressing them at a pressure of 11 metric tonnes into discs 12.5 mm in diameter and 2 mm thick. Waveguide films were made by drop-casting many small drops of either a methanol or acetone solution onto a metal plate. The entire waveguide plate was

then uniformly covered by a thin liquid layer with a volume of 50 to 100 μL of solution, aided by the good wetting of these methanol and acetone solutions on the metal. The thicker edges of the drop-cast films were removed with a solvent-soaked swab, resulting in visually uniform films.

The crystalline morphology and quality of the thin film has been observed to depend on the metal substrate. This is probably related to the chemical interaction between the metal and the first layer of the deposited film. The morphology of subsequent layers of the film is then dependent on the morphology of this first layer. The presence of high quality crystalline films is critical for waveguide THz-TDS. Initially, the sample was drop-cast on an optically polished, plasma-cleaned Cu waveguide plate. If acceptable waveguide THz-TDS spectra could not be obtained, the sample was drop-cast on an optically polished, plasma-cleaned Al waveguide plate. If acceptable waveguide THz-TDS spectra could still not be obtained, the sample was then drop-cast on a soft-brush finished, plasma-cleaned Al waveguide plate. Both the crystal morphology and the waveguide spectra clearly depended on the metal substrate, and in some cases, the surface finish of the substrate. The acceptability of the sample was determined by comparing the room-temperature spectra to that of the pellet and by observing the behavior of the spectra upon cooling. An acceptable room-temperature spectrum would have features at similar frequencies compared to the corresponding pellet. Since intermolecular vibrational modes are critically dependent on crystal morphology, if the pellet and waveguide have similar spectra they should also have the same polymorph. In addition, spectral features that do not change upon cooling tend to be due to scattering from the polycrystalline film and are associated with unacceptable films.

Optical micrographs of the five investigated waveguide films are shown in Fig. 4. The sizes of the observed crystals range from approximately 10 μm to 100 μm. The planar order of the salicylic acid, 3-hydroxybenzoic acid, 4-hydroxybenzoic acid, and aspirin is apparent to the eye. The ability of the drop-casting technique to create polycrystalline films with planar order has been previously demonstrated via optical micrographs of many materials[16,17] and by X-ray analysis of drop-cast films of TCNQ.[16]

For the measurements, the THz pulses transmitted through the sample pellet or the thin film coated waveguide were measured at 295 K and 77 K, as shown in Figs. 1 and 2, respectively. The corresponding amplitude spectra were then calculated via a numerical Fourier transform. A reference was obtained by fitting the spectrum to a spline away from any absorption features. The amplitude absorbance was determined from this reference $A_R(\omega)$ and the transmitted amplitude spectrum $A_T(\omega)$ was determined by the following relationship: Absorbance $= -\ln [A(\omega)_T/A(\omega)_R]$. While this calculated absorbance does not include any broadband absorbance, it does accurately determine the center frequencies and linewidths of any sharp features.

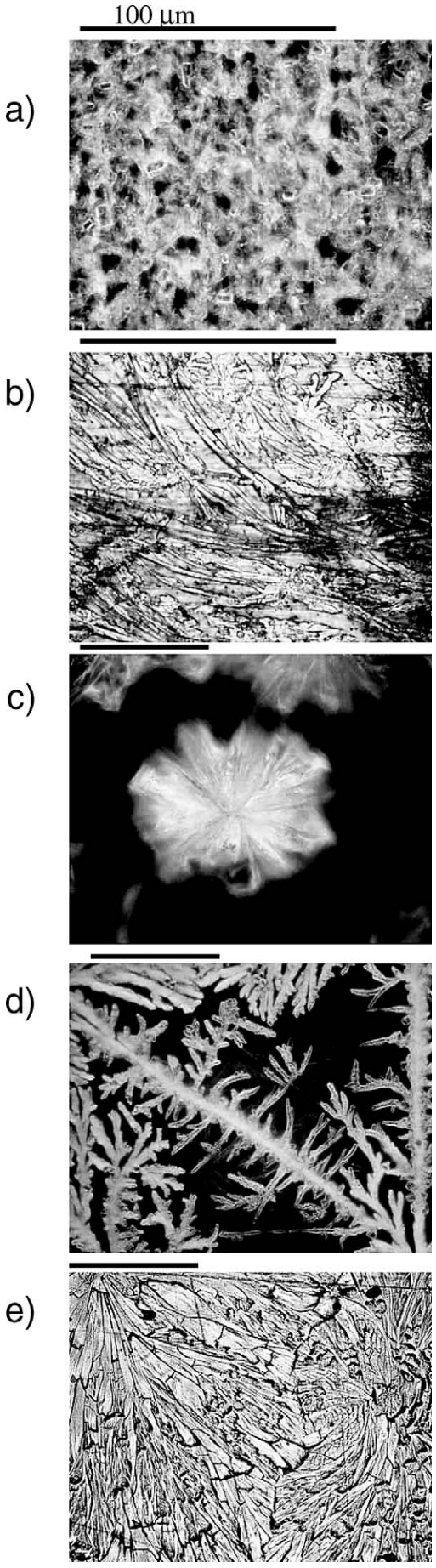

→

FIG. 4. Optical micrographs of measured polycrystalline films on metal waveguide plates. Horizontal lines correspond to 100 μm. (**a**) Benzoic acid film on brushed Al plate. (**b**) Salicylic acid film on polished Cu plate. (**c**) 3-Hydroxybenzoic acid film on polished Al plate, image is negative for clarity. (**d**) 4-Hydroxybenzoic acid film on polished Al plate, image is negative for clarity. (**e**) Aspirin film on polished Cu plate.

TABLE I. Absorbance line frequencies and FWHM line widths (in parentheses) in THz at 77 K.

Benzoic acid		Salicylic acid		3-Hydroxy-benzoic acid		4-Hydroxy-benzoic acid		Aspirin	
Pellet	Waveguide	Pellet	Waveguide	Pellet	Waveguide	Pellet	Waveguide	Pellet	Waveguide
	0.73 (0.02)	1.21 (0.05)	1.23 (0.04)	0.88 (0.04)	0.89 (0.04)	1.96 (0.10)	1.99 (0.06)		1.11 (0.05)
1.03 (0.07)	1.05 (0.03)	1.53 (0.04)	1.55 (0.03)	0.94 (0.04)	0.96 (0.04)	2.09 (0.08)	2.12 (0.07)	1.68 (0.25)	1.87 (0.06)
1.20 (0.06)	1.21 (0.03)	1.77 (0.05)	1.79 (0.06)	2.06 (0.05)	2.08 (0.04)		2.46 (0.14)	2.14 (0.37)	2.17 (0.06)
2.07 (0.12)	2.09 (0.06)	2.00 (0.07)	2.04 (0.07)		2.26 (0.08)		3.22 (0.06)		2.35 (0.11)
2.38 (0.10)	2.34 (0.07)	2.21 (0.10)	2.25 (0.07)	2.34 (0.07)	2.36 (0.05)				2.49 (0.05)
2.68 (0.11)	2.74 (0.08)	2.39 (0.06)	2.42 (0.04)						2.87 (0.12)
2.92 (0.07)	2.96 (0.07)	2.52 (0.12)	2.56 (0.07)						3.34 (0.23)
	3.16 (0.11)	2.91 (0.10)							3.69 (0.11)
	3.73 (0.11)								

RESULTS

A summary of the observed absorbance line frequencies and linewidths for both pellets and waveguide films of these materials at 77 K is shown in Table I. All of these materials have been examined previously by Walther et al.[19,20] using pellets, while benzoic acid has been examined in both pellets and single crystals by Zelsmann[21] and aspirin has been examined in powder form at room temperature by Kawase[8] and with FT-IR by Boczar.[22] We will now discuss these materials individually in more detail.

The benzoic acid waveguide film was prepared by drop casting a 5 mg/mL acetone solution onto a brushed Al plate, while the corresponding pellet was a 28:330 mg mixture of analyte to polyethylene. It is to be noted that resolved spectral lines could not be obtained on either polished Cu or polished Al plates. At room temperature, both the waveguide and pellet have similar spectra, with three observed features at 0.90, 1.10, and 1.93 THz. However, upon cooling to 77 K, the pellet features only sharpened slightly, while the corresponding features of the waveguide sharpened up significantly (see Fig. 5), revealing nine lines with full width at half-maximum (FWHM) widths ranging from 20 to 110 GHz. Linewidths for the waveguide spectra are typically on the order of one-half the corresponding linewidth for the pellet (with the exception of the 2.92 THz line). All of these lines have been observed in Refs. 19–21, albeit at much lower temperatures. Indeed, the linewidths seen in our technique compare favorably with single crystal measurements taken at 6 K.[21]

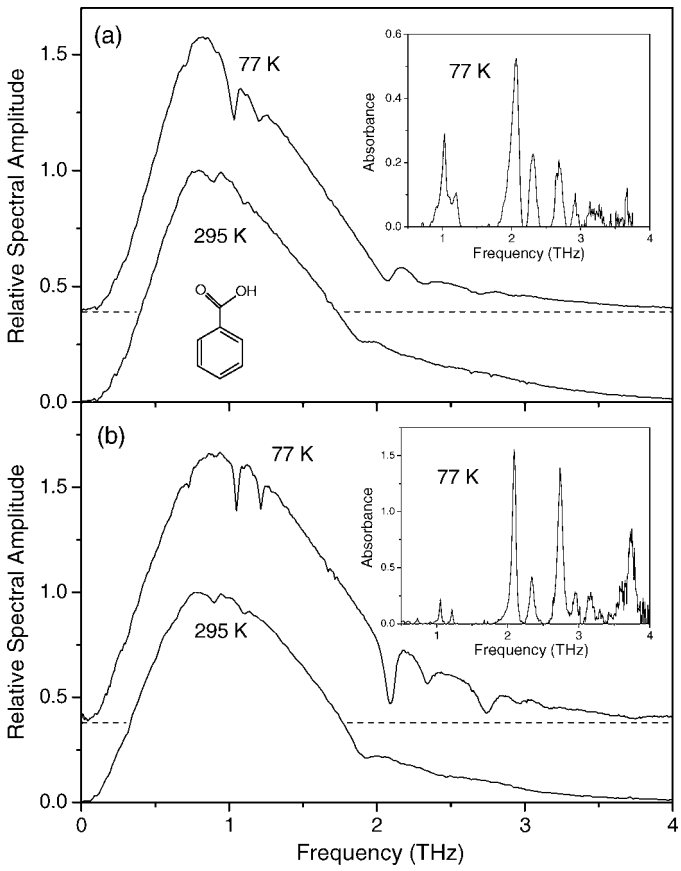

FIG. 5. THz spectra transmitted (**a**) through benzoic acid pellet and (**b**) through waveguide with benzoic acid film. Spectra at 77 K are offset for clarity. Insets show absorbance spectra at 77 K. Spectra at 295 K are normalized to unity.

These absorption lines have been tentatively assigned[19–21,23,24] to different vibrational modes. The lowest three lines (0.73 through 1.21 THz) have been assigned to external translations of the benzoic acid dimers within the crystal. The other observed lines (2.09 through 3.73 THz) have been assigned to intermonomer (i.e., hydrogen bonded) modes mixed with twisting of the carbonyl group. Reference 21 has specifically assigned these lines to intermonomer torsion, bending, and stretching.

The salicylic (2-hydroxybenzoic) acid waveguide film was prepared by drop casting a 10 mg/mL acetone solution onto a polished Cu plate, while the corresponding pellet was a 27:330 mg mixture of analyte to polyethylene. Here, the cooled waveguide reveals seven features with linewidths ranging from 40 to 80 GHz. In particular, with the pellet the four features between 2.0 and 2.5 THz overlap somewhat, while with the waveguide they are distinct (see Fig. 6). This is due to the lines at 2.2 and 2.5 THz with the waveguide having a linewidth approximately one-half the value of the corresponding line in the pellet. Note that while the apparent linewidth of the 1.79 THz line has increased with the waveguide, the reduced intensity makes an accurate measurement of this particular linewidth difficult.

The relative intensities of the absorption lines differ between the pellet and the waveguide. This is likely due to the planar ordering of the microcrystals on the metal surface, resulting in the electric dipoles associated with the absorption lines having a given orientation with respect to the THz electric field within the waveguide, in contrast to random orientations for the pellet. In particular, the 2.2 THz line is strongly enhanced for the waveguide, while the 2.9 THz line has vanished, suggesting that the corresponding dipole is along the waveguide surface

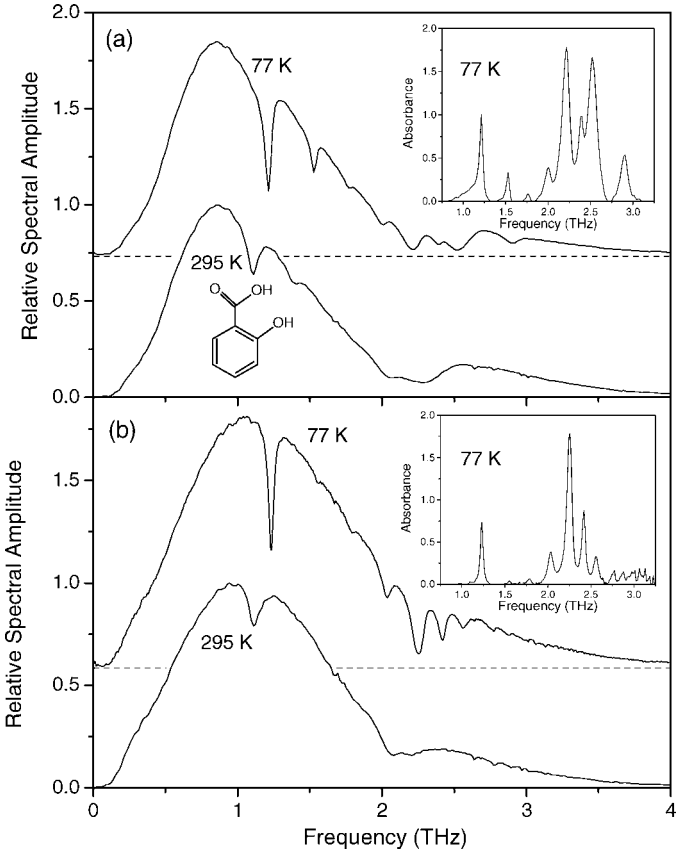

FIG. 6. THz spectra transmitted (**a**) through salicylic acid pellet and (**b**) through waveguide with salicylic acid film. Spectra at 77 K are offset for clarity. Insets show absorbance spectra at 77 K. Spectra at 295 K are normalized to unity.

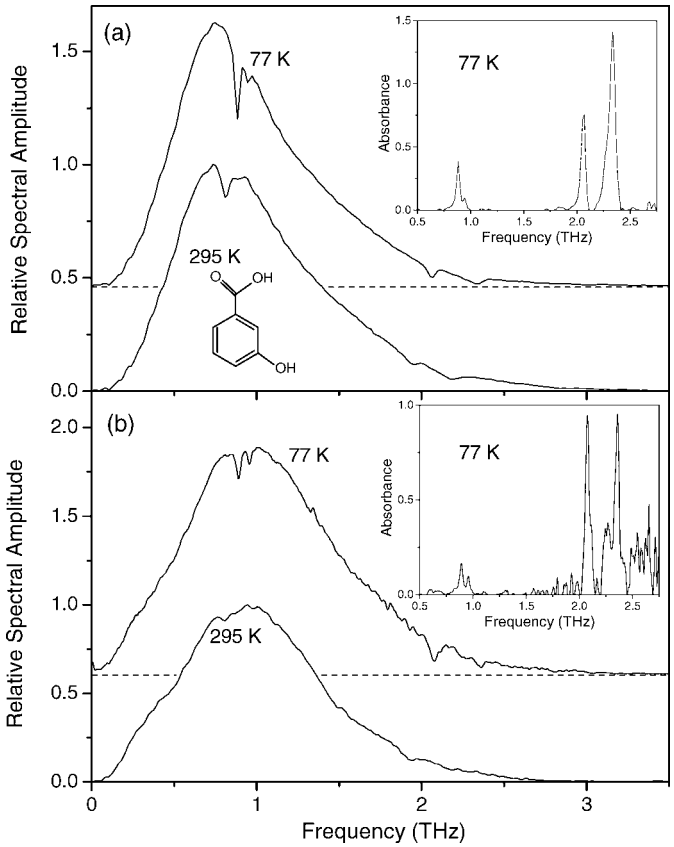

FIG. 7. THz spectra transmitted (**a**) through 3-hydroxybenzoic acid pellet and (**b**) through waveguide with 3-hydroxybenzoic acid film. Spectra at 77 K are offset for clarity. Insets show absorbance spectra at 77 K. Spectra at 295 K are normalized to unity.

(i.e., perpendicular to the THz electric field). All of the observed lines have been seen earlier with pellets in Ref. 19 at temperatures down to 10 K. However, even at these low temperatures, nearly all of the pellet absorption lines are broader than our waveguide absorption lines at 77 K. Similarly to benzoic acid, the three lowest frequency lines have been assigned[20] to external translations of the dimers, while the higher frequency lines have been assigned to intermonomer vibrations. The 2.26 THz line has been specifically assigned[25] to a rocking motion of the monomers.

The 3-hydroxybenzoic acid waveguide film was prepared by drop casting a 23 mg/mL acetone solution onto a polished Al waveguide plate, while the corresponding pellet was a 27:330 mg mixture of analyte to polyethylene. The cooled pellet revealed four features (see Fig. 7a). The highest frequency line is slightly narrower for the cooled waveguide (see Fig. 7b), revealing that it is actually a doublet, resulting in a total of five lines with line widths ranging from 40 to 80 GHz. The noise in the waveguide spectrum is not random, but is due to the scattering from inhomogeneities in the polycrystalline film. As seen in Fig. 4c, the 3-hydroxybenzoic acid film is composed of large ($\sim$100 μm) crystal clusters with similar sizes and planar order, but random positions along the metal surface. These introduce scattering while still minimizing inhomogeneous broadening. Surprisingly, while the pellet and waveguide spectra are in agreement with each other, neither is in agreement with previous work by Walther.[19,20] We are not aware of any other published work on this molecule at these frequencies. We have repeated our experiments with 3-hydroxybenzoic acid from another supplier (Acros) with the same results.

The 4-hydroxybenzoic acid waveguide film was prepared by drop casting a 10 mg/mL methanol solution onto a polished Al waveguide plate, while the corresponding pellet was a 27:330 mg mixture of analyte to polyethylene. The cooled pellet shows two absorption lines while the cooled waveguide reveals four absorption lines (see Fig. 8). The low-frequency wing of the lowest frequency absorption line is reduced significantly with the waveguide, compared to the pellet. All of these absorption lines, with the exception of the line at 2.46 THz, have been observed previously in Ref. 19. Both 3- and 4-hydroxybenzoic acid have very different spectra compared to salicylic acid (2-hydroxybenzoic acid), illustrating the ability of waveguide THz-TDS (and THz-TDS in general) to clearly distinguish between isomorphs.

Finally, the aspirin waveguide was prepared by drop casting a 27 mg/mL methanol solution onto a polished Cu waveguide plate, while the corresponding pellet was a 28:330 mg mixture of analyte to polyethylene. Here, there is substantial line narrowing for the waveguide film, especially compared to the pellet. The pellet only has two very broad features at 77 K (see Fig. 9a), while with the waveguide, these two broad features are clearly resolved into eight narrow features with linewidths ranging from 50 to 230 GHz (see Fig. 9b). The linewidths with the waveguide are approximately four times narrower than the corresponding lines with the pellet. All of the lines have been

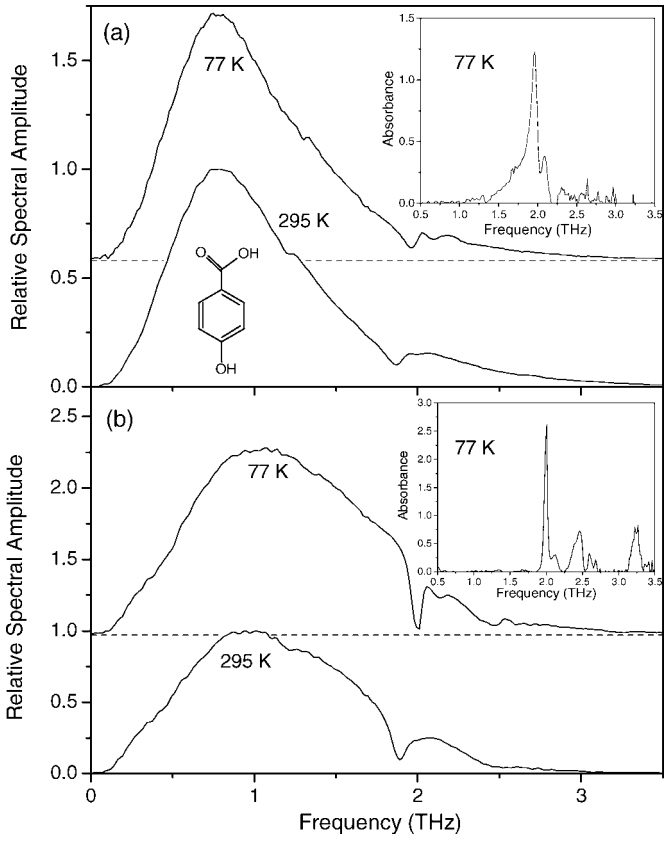

FIG. 8. THz spectra transmitted (**a**) through 4-hydroxybenzoic acid pellet and (**b**) through waveguide with 4-hydroxybenzoic acid film. Spectra at 77 K are offset for clarity. Insets show absorbance spectra at 77 K. Spectra at 295 K are normalized to unity.

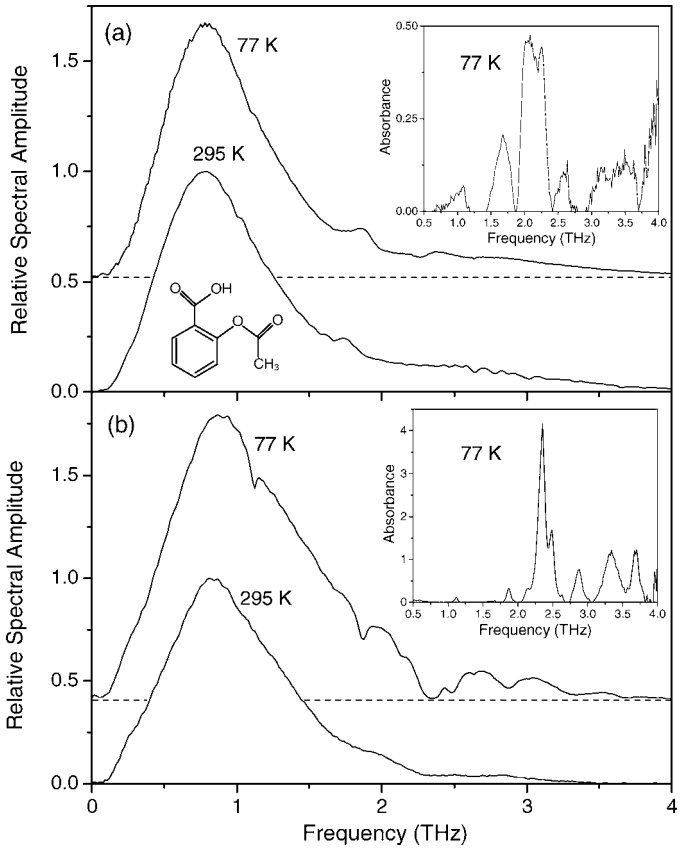

FIG. 9. THz spectra transmitted (**a**) through aspirin pellet and (**b**) through waveguide with aspirin film. Spectra at 77 K are offset for clarity. Insets show absorbance spectra at 77 K. Spectra at 295 K are normalized to unity.

seen previously in Ref. 20, albeit with considerably different relative amplitudes and at much lower temperatures.

The infrared and THz spectrum of an isolated aspirin dimer has been calculated theoretically in Ref. 22. While the THz vibrational modes of crystalline materials tend to be strongly affected by the crystal structure and have a significant external (phonon) character,[26] two of the features predicted by Ref. 22 agree with our experimental results. The calculated frequencies of these features are 2.19 and 3.39 THz (corresponding to our features at 2.17 and 3.34 THz) and correspond to the torsion of both the carboxyl and acetyl groups and to the torsion of the methyl group, respectively. Waveguide THz-TDS can provide the precise, high-resolution experimental spectrum which may guide this ongoing theoretical study.[22]

CONCLUSION

The preceding five examples show how the power and utility of waveguide THz-TDS can be applied to pharmaceutical materials such as aspirin and related materials. The line-narrowing is particularly pronounced with benzoic acid and aspirin. The increased resolution may allow one to obtain more detailed and precise information about the vibrational modes of these materials and their associated structural conformations. The increased resolution would also help in establishing a precise spectral fingerprint, which may assist in their identification. In essence, waveguide THz-TDS allows one to obtain spectra that rival single crystal measurements, but with easier to form polycrystalline films. In addition, even for non-crystalline films, waveguide THz-TDS has improved sensitivity compared to conventional THz-TDS by approximately a factor of 100, allowing one to identify smaller quantities. This combination of both high resolution and sensitivity, together with relatively simple sample preparation, shows promise for the study and precise identification of the vibrational modes of pharmaceutical materials.

ACKNOWLEDGMENTS

We would like to thank Architha Nath for technical support concerning the sample preparation and Joseph S. Melinger for useful discussions. This work was partially supported by the National Science Foundation.

1. P. F. Taday, I. V. Bradley, D. D. Arnone, and M. Pepper, J. Pharm. Sci. **92,** 831 (2003).
2. C. J. Strachan, T. Rades, D. A. Newnham, K. C. Gordon, M. Pepper, and P. F. Taday, Chem. Phys. Lett. **390,** 20 (2004).
3. C. J. Strachan, P. F. Taday, D. A. Newnham, K. C. Gordon, J. A. Zeitler, M. Pepper, and T. Rades, J. Pharm. Sci. **94,** 837 (2005).
4. J. A. Zeitler, D. A. Newnham, P. F. Taday, T. L. Threlfall, R. W. Lancaster, R. W. Berg, C. J. Strachan, M. Pepper, K. C. Gordon, and T. Rades, J. Pharm. Sci. **95,** 2486 (2006).
5. J. A. Zeitler, D. A. Newnham, P. F. Taday, C. J. Stracham, M. Pepper, K. C. Gordon, and T. Rades, Thermochimica Acta **436,** 71 (2005).
6. P. F. Taday, Phil. Trans. R. Soc. Lond. A **362,** 351 (2004).
7. B. Fischer, M. Hoffmann, H. Helm, G. Modjesch, and P. U. Jepsen, Semicond. Sci. Technol. **20,** S246 (2005).
8. K. Kawase, Y. Ogawa, Y. Watanabe, and H. Inoue, Opt. Exp. **11,** 2549 (2003).
9. M. Lu, J. Shen, N. Li, Y. Zhang, C. Zhang, L. Liang, and X. Xu, J. Appl. Phys. **100,** 103104 (2006).
10. J. Zhang and D. Grischkowsky, Opt. Lett. **19,** 1617 (2004).

11. J. S. Melinger, N. Laman, S. S. Harsha, and D. Grischkowsky, Appl. Phys. Lett. **89,** 251110 (2006).
12. D. Grischkowsky, S. Keiding, M. van Exter, and Ch. Fattinger, J. Opt. Soc. Am. B **7,** 2006 (1990).
13. M. van Exter and D. Grischkowsky, IEEE Trans. on Microwave Theory Technol. **38,** 1684 (1990).
14. G. Gallot, S. P. Jamison, R. W. McGowan, and D. Grischkowsky, J. Opt. Soc. Am. B **17,** 851 (2000).
15. R. Mendis and D. Grischkowsky, Opt. Lett. **26,** 846 (2001).
16. J. S. Melinger, N. Laman, S. S. Harsha, S. F. Cheng, and D. Grischkowsky, J. Phys. Chem. A **111,** 10977 (2007).
17. N. Laman, S. S. Harsha, D. Grischkowsky, and J. S. Melinger, "High resolution waveguide THz spectroscopy of biological molecules", Biophys. J., paper in press (2008).
18. N. Laman and D. Grischkowsky, Appl. Phys. Lett. **90,** 122115 (2007).
19. M. Walther, P. Plochocka, B. Fischer, H. Helm, and P. U. Jepsen, Biopolymers **67,** 310 (2002).
20. M. Walther, Ph.D. Thesis, Albert-Ludwigs-Universität, Freiburg, Germany (2003).
21. H. R. Zelsmann and Z. Mielke, Chem. Phys. Lett. **186,** 501 (1991).
22. M. Boczar, M. Wójcik, K. Szczeponek, D. Jamróz, A. Zięba, and B. Kawałek, Chem. Phys. **286,** 63 (2003).
23. G. Klausberger, K. Furić, and L. Colombo, J. Raman Spectrosc. **6,** 277 (1977).
24. M. Plazanet, N. Fukushima, M. R. Johnson, A. J. Horsewill, and H. P. Trommsdorff, J. Chem. Phys. **115,** 3241 (2001).
25. M. Boczar, Ł. Boda, and M. Wójcik, J. Chem. Phys. **124,** 084306 (2006).
26. P. U. Jepsen and S. J. Clark, Chem. Phys. Lett. **442,** 275 (2007).